

The Role of Dissociative Electron Attachment in Focused Electron Beam Induced Processing: A Case Study on Cobalt Tricarbonyl Nitrosyl**

Sarah Engmann, Michal Stano, Štefan Matejčík,* and Oddur Ingólfsson*

Motivated by the potentially adverse effects of dissociative electron attachment (DEA) in focused electron beam induced processing (FEBIP), we have conducted a gas-phase DEA study on the common FEBIP precursor molecule, cobalt tricarbonyl nitrosyl. We have determined the absolute DEA cross-sections and the branching ratios for the individual fragmentation processes in the energy range from about 0–9 eV. We further report the adiabatic electron affinities (EAs) of the corresponding neutral radicals. Finally, we propose a fragmentation mechanism, which we believe is valid for DEA to metal–carbonyl compounds in general.

Initially discovered as an unwelcome side effect in electron microscopy,^[1] FEBIP has quickly been embraced as a clean and precise tool for manipulating and controlling matter on a small scale. A focused, high-energy electron beam is used to locally dissociate adsorbed precursor molecules. Ideally, a chemically and structurally well-defined deposit is left behind while volatile fragments are pumped away. Minimization of the spatial resolution and eliminating contamination of the deposited structures remain the two main challenges of FEBIP.^[2,3]

Albeit a highly focused primary electron beam, the width of the deposits is typically a multiple of the incident beam diameter.^[4] Elastic and inelastic scattering events are unavoidable when irradiating samples with high-energy electron beams. Consequently, secondary (SE) and back-scattered electrons (BSE) are emitted from the sample surface and the deposit, creating electron flux outside the focus point of the primary beam. Simulations as well as experiments show that the SE energy distribution typically peaks at low energies, that is, < 15 eV, and their intensities are far from negligible.^[2,4,5]

At these low energies, a new fragmentation pathway becomes available, that is, DEA. In contrast to fragmentation by direct electron impact, where excess energy of several electron volts is required, DEA can occur close to zero eV threshold. Furthermore, DEA reactions can exhibit fairly large cross-sections of 10^{-18} to 10^{-16} m² and are highly bond selective with regards to the electron energy.^[6,7]

Because of the abundance of low-energy SEs and BSEs generated in FEBIP and the potentially high cross-sections, DEA may play a significant role in FEBIP broadening. Additionally, the high bond selectivity in DEA may contribute to the deposition of incompletely decomposed precursor molecules and thus to an increased nonmetallic fraction of the deposit. Presently, no DEA cross-section data has been reported on relevant FEBIP precursor molecules and current simulations either neglect dissociation caused by low-energy electrons altogether or have to rely on an educated guess for the cross-sections.^[4]

Herein we report absolute DEA cross-sections and branching ratios for cobalt tricarbonyl nitrosyl. We report the electron affinities for the neutral radical fragments and we propose a general DEA mechanism for metal–carbonyl compounds.

The present experiments were performed in a crossed electron/molecular beam apparatus^[8] under single collision conditions. The molecular beam was generated by gas effusion through a stainless steel capillary and the pressure was monitored with an absolute capacitance gauge (MKS Baratron, 0–7 Pa). The electron beam (full width at half maximum, FWHM, of 140 meV) was generated by a trochoidal electron monochromator and the energy scale was calibrated relative to the formation of SF₆[−] from SF₆ at an electron energy of 0 eV. Absolute cross-sections were estimated relative to the cross-section of SF₅[−]/SF₆ at 300 K.^[9] In the mass range studied, the transmission through the quadrupole and the detection efficiency should not vary much. However, the ion extraction field is fairly low (1 V cm^{−1}) and ions formed with high kinetic energy may thus escape collection. This is likely to be the main source of error, and though the kinetic energy is not likely to be substantial in the fragmentation processes studied, it is adequate to look at these cross-sections as a lower limit. Conservatively, we estimate the absolute errors to be about a factor of two. Cobalt tricarbonyl nitrosyl was purchased from Strem Chemicals (Bischheim, France) and used as received.

Figure 1 shows the energy dependence of the DEA cross-sections for the formation of the individual negative ion fragments. The fragmentation pattern is characterized by the

[*] S. Engmann, Prof. Dr. O. Ingólfsson
 Science Institute and Department of Chemistry
 University of Iceland, Dunhagi 3, 107 Reykjavík (Iceland)
 E-mail: odduring@hi.is

Dr. M. Stano, Prof. Dr. Š. Matejčík
 Department of Plasma Physics, Comenius University
 Mlynska dolina F2, 84248 Bratislava (Slovakia)
 E-mail: stefan.matejcik@fmph.uniba.sk

[**] This work was supported by the Icelandic Centre for Research (RANNIS) and the Slovak grants (VEGA 1/0558/09 and APVV-0365-07). S.E. acknowledges a PhD grant from the University of Iceland and a travel grant from the COST Action (grant number CM0601, ECCL). We thank P. Klüpfel for help with the fitting procedures.

Supporting information for this article is available on the WWW under <http://dx.doi.org/10.1002/anie.201103234>.

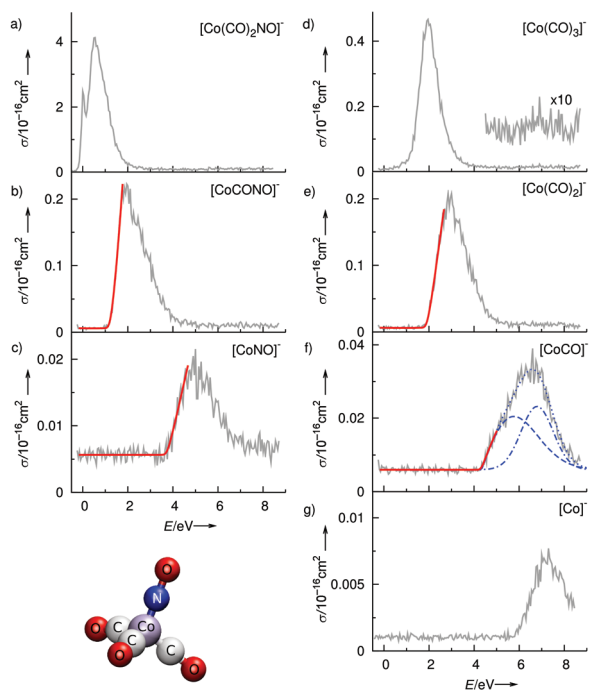


Figure 1. DEA cross-sections for individual fragment formation from $[\text{Co}(\text{CO})_3\text{NO}]^-$ as a function of incident electron energy. The threshold fit functions are given as solid red lines (b, c, e, and f), and the Gaussian-type fit functions indicate the two contributions to the yield of $[\text{CoCO}]^-$ (blue dotted lines, f).

loss of one or more CO units (Figure 1 a–c), the loss of one NO unit (Figure 1 d), or the loss of one NO and one or more CO units (Figure 1 e–g). The most prominent channel is the formation of $[\text{Co}(\text{CO})_2\text{NO}]^-$ through cleavage of one CO unit from the parent molecular anion (Figure 1 a). This channel shows a narrow contribution close to 0 eV in the ion yield curve and a broader one that peaks close to 1 eV. Based on the commonly measured high cross-sections for DEA processes close to 0 eV, and the fact that the population of energy levels $v=1$ and $v=2$ of the symmetric Co–CO stretch vibration ($\nu=390\text{ cm}^{-1}$)^[10] at room temperature is about 15.4 and 2.5 %, respectively, we assign the narrow contribution close to 0 eV to hot-band transitions. For the formation of $[\text{Co}(\text{CO})_2\text{NO}]^-$ at its maximum of around 1 eV, we estimate the cross-section to be close to $4 \times 10^{-16}\text{ cm}^2$. The second most prominent channel in DEA to $[\text{Co}(\text{CO})_3\text{NO}]^-$ is the formation of $[\text{Co}(\text{CO})_3]^-$, that is, the loss of the NO ligand (Figure 1 d). This decay channel peaks close to 2 eV and we estimate the cross-section to be close to $5 \times 10^{-17}\text{ cm}^2$. The further loss of a CO ligand from $[\text{Co}(\text{CO})_2\text{NO}]^-$ and $[\text{Co}(\text{CO})_3]^-$, respectively, is in both cases characterized by a broad peak in the respective ion yield curve, shifted by approximately 1 eV with regards to the precursor. Both of these peaks are highly asymmetric with a sharp rise at the low-energy side but a smoother, Gaussian-like, decay on the high-energy side. We estimate the cross-section for both of these processes to be close to $2 \times 10^{-17}\text{ cm}^2$ at the respective maxima. The loss of one more CO ligand to form $[\text{CoNO}]^-$ takes place in the energy range from 4–7 eV and has its maximum close to 5 eV.

The contribution from $[\text{CoCO}]^-$, on the other hand, stretches from 4–8 eV, peaks between 6 and 7 eV and has a clear shoulder at the low-energy side. The cross-section for these processes is estimated to be 2×10^{-18} and $4 \times 10^{-18}\text{ cm}^2$ at the respective maxima. Finally, Co^- stripped of all ligands is observed through a high-energy resonance centered slightly above 7 eV with a maximum cross-section of about $7 \times 10^{-19}\text{ cm}^2$. The parent anion $[\text{Co}(\text{CO})_3\text{NO}]^-$ is not discernible under the present experimental conditions.

The UV/Vis absorption spectrum of $[\text{Co}(\text{CO})_3\text{NO}]^-$ consists of two broad bands centered around 380 nm (around 3.3 eV) and 210 nm (around 5.9 eV), respectively.^[11] Photodissociation studies at excitation wavelengths close to the first maximum of 355 nm (around 3.5 eV) indicate loss of both CO and NO ligands. Generally, the photodissociation mechanism of metal–carbonyl compounds is understood as an initial photoexcitation to a repulsive state, causing loss of the first ligand. Internal redistribution of the excess energy then leads to further sequential ligand loss.^[11,12] The fragmentation mechanism observed in our DEA study can be explained in a similar manner. Here, the initial step at low energies is the formation of a single-particle shape-resonance, which peaks at 1 eV and predominantly decays by loss of a CO ligand. The contribution at about 2 eV, on the other hand, that also results in NO loss, is tentatively assigned to a low-lying core-excited resonance, which corresponds to the band observed at 380 nm (3.3 eV) in the UV/Vis region. Hence, this resonance is correlated with the HOMO–LUMO transition, but in DEA the ion yield is shifted towards lower electron energies because of the competition of autodetachment from the transient negative ion (TNI). In both cases an initial occupation of a previously empty MO causes direct bond rupture and the shape of the ion yield curves for $[\text{Co}(\text{CO})_2\text{NO}]^-$ and $[\text{Co}(\text{CO})_3]^-$ are governed by the formation and survival probability of the respective TNI. After this initial dissociation step, however, the excess energy is redistributed within the remaining anion fragment and further, statistical dissociation takes place. The loss of the second (and third) ligand is thus governed by the energetics and not the initial formation probability of the respective TNIs. This is evident by the steep threshold for the loss of CO from $[\text{Co}(\text{CO})_3]^-$ and $[\text{Co}(\text{CO})_2\text{NO}]^-$ (Figure 1 b,e). This also applies to the formation of the Co^- anion, although, in this case, we assign the initial step to the formation of a core-excited resonance, which probably corresponds to the band at 210 nm in the UV/Vis spectrum. We draw this conclusion from the threshold behavior and the shape of the ion yield as well as the fact that this resonance contributes significantly to the yield of $[\text{CoCO}]^-$ (see Gaussian fits in Figure 1 f and the Supporting Information) but is absent in the yield of $[\text{CoNO}]^-$. Hence, this resonance must initially decay by loss of NO before further statistical fragmentation leads to $[\text{CoCO}]^-$ and finally Co^- . As statistical decay strongly depends on the time scale of the experiment it would be interesting to further verify the proposed mechanism with a complimentary study on the time dependency of the individual processes.

Independent of the process, the DEA thermochemical threshold, $E_{\text{th}}(\text{X}^-)$, is given by Equation (1),

$$E_{\text{th}}(\text{X}^-) = \sum_{m=1}^n \text{BDE}(\text{X} - \text{Y}_m) - \text{EA}(\text{X}) \quad (1)$$

where X is the observed charged fragment and $\text{Y}_1 \dots \text{Y}_n$ are the dissociated ligands. Using the vertical detachment energy of 1.73 eV as the electron affinity (EA) for the $[\text{Co}(\text{CO})_2\text{NO}]$ radical,^[13] and the average Co–CO bond dissociation energy (BDE) of 1.42 eV derived from $[\text{Co}(\text{CO})_4]$,^[14,15] the loss of the first CO becomes energetically available at about –0.3 eV. Hence, the loss of the first CO is an exothermic process. In a similar way, an estimated threshold energy of 0.2 eV for the formation of $[\text{Co}(\text{CO})_3]^-$ and a Co–NO binding energy of 1.89 eV^[15] leads to an EA value of about 1.7 eV for $[\text{Co}(\text{CO})_3]$. For the higher-order dissociation channels the sharp onset allows for more accurate determination of the threshold by fitting the data to an empirical threshold law commonly used for collision-induced dissociation data (see the Supporting Information). These fits give us threshold values of 1.9 and 1.2 eV for further CO loss from $[\text{Co}(\text{CO})_3]^-$ and $[\text{Co}(\text{CO})_2\text{NO}]^-$, respectively, and values of 4.3 and 3.7 eV for CO loss from $[\text{Co}(\text{CO})_2]^-$ and $[\text{Co}(\text{CO})\text{NO}]^-$. Using the previously stated BDEs, we estimate the following adiabatic electron affinities from Equation (1): $\text{EA}([\text{Co}(\text{CO})\text{NO}]) = 1.6$ eV, $\text{EA}([\text{Co}(\text{CO})_2]) = 1.4$ eV, $\text{EA}([\text{CoNO}]) = 0.5$ eV, and $\text{EA}([\text{CoCO}]) = 0.4$ eV. These values and our estimate for the electron affinity of $[\text{Co}(\text{CO})_3]$ are in very good agreement with the previously limiting EA values, that is, $1.35 \text{ eV} < \text{EA}([\text{Co}(\text{CO})_2]) < \text{EA}([\text{Co}(\text{CO})\text{NO}]) < \text{EA}([\text{Co}(\text{CO})_3]) < \text{EA}([\text{Co}(\text{CO})_2\text{NO}]) = 1.73$.^[13]

The DEA cross-sections reported here for $[\text{Co}(\text{CO})_3\text{NO}]$ range from 10^{-16} – 10^{-19} cm^2 and DEA predominantly leads to incomplete decomposition of the parent molecule. Considering that the yield of SEs can be close to 0.1 SEs per primary electron per electron volt,^[2] the effect of DEA is not negligible and partial decomposition through DEA might

even contribute significantly to nonmetallic contamination. Further DEA cross-section studies on different FEBIP precursors should be valuable in conjunction with simulation to map the influence of different metal/ligand compositions. Eventually this information can be used to design precursor molecules that enable improved resolution and purer deposits.

Received: May 11, 2011

Published online: August 25, 2011

Keywords: carbonyl ligands · cobalt · cross-sections · dissociative electron attachment · gas-phase reactions

- [1] A. Ennos, *Br. J. Appl. Phys.* **1953**, 4, 101.
- [2] I. Utke, P. Hoffmann, J. Melngailis, *J. Vac. Sci. Technol. B* **2008**, 26, 1197, and references therein.
- [3] W. F. van Dorp, C. W. Hagen, *J. Appl. Phys.* **2008**, 104, 081301.
- [4] N. Silvis-Cividjian, C. W. Hagen, P. Kruit, *J. Appl. Phys.* **2005**, 98, 084905, and references therein.
- [5] J. Schäfer, J. Hölzl, *Thin Solid Films* **1972**, 13, 81.
- [6] L. G. Christophorou, J. K. Olthoff, *Appl. Surf. Sci.* **2002**, 192, 309.
- [7] I. Bald, J. Langer, P. Tegeder, O. Ingólfsson, *Int. J. Mass Spectrom.* **2008**, 277, 4.
- [8] M. Stano, Š. Matejčík, J. D. Skalny, T. D. Märk, *J. Phys. B* **2003**, 36, 261.
- [9] M. Braun, S. Marienfeld, M.-W. Ruf, H. Hotop, *J. Phys. B* **2009**, 42, 125202.
- [10] R. S. McDowell, W. D. Horrocks, Jr., J. T. Yates, *J. Chem. Phys.* **1961**, 34, 530.
- [11] S. Georgiou, C. A. Wight, *J. Chem. Phys.* **1989**, 90, 1694.
- [12] W. H. Wang, F. H. Chen, J. G. Lin, Y. B. She, *J. Chem. Soc. Faraday Trans.* **1995**, 91, 847.
- [13] N. J. Turner, A. A. Martel, I. M. Waller, *J. Phys. Chem.* **1994**, 98, 474, and references therein.
- [14] J. A. Connor, *Top. Curr. Chem.* **1977**, 71, 72.
- [15] J. Opitz, *Int. J. Mass Spectrom.* **2003**, 225, 115.